

ORIGINAL ARTICLE

# Electro-acupuncture Pretreatment at Zusanli (ST36) Acupoint Attenuates Lipopolysaccharide-Induced Inflammation in Rats by Inhibiting $\text{Ca}^{2+}$ Influx Associated with Cannabinoid CB2 Receptors

Tao Chen,<sup>1</sup> Yong Xiong,<sup>2</sup> Man Long,<sup>3</sup> Dan Zheng,<sup>1</sup> Hui Ke,<sup>1</sup> Jun Xie,<sup>2</sup> Nina Yin,<sup>1,5</sup> and Zebin Chen<sup>4,5</sup>

**Abstract—** In this study, we aimed to investigate the effect of electro-acupuncture (EA) pretreatment at zusanli (ST36) acupoint on lipopolysaccharide (LPS)-induced endotoxemic rat model and explore the underlying molecular mechanisms. Rats were treated with EA at ST36 for 7 days before being subjected to LPS. Two hours post-LPS, samples such as serum, local acupoint tissues, and spleens were collected and processed for investigations including cytokine production, cytosolic calcium ( $\text{Ca}^{2+}$ ) concentration,  $\text{Ca}^{2+}$  influx, cannabinoid CB2 receptor (CB2R) expression, and TLR4/NF- $\kappa$ B signaling. Our results showed EA pretreatment significantly attenuated LPS-induced inflammatory cytokine production, such as TNF- $\alpha$ , IL-1 $\beta$ , and IL-6. EA also enhanced CB2R expression, inhibited  $\text{Ca}^{2+}$  influx, and inactivated TLR4/NF- $\kappa$ B signaling, subsequently resulting in a substantial reduction of  $\text{Ca}^{2+}$  concentration. Importantly, CB2R antagonist AM630 effectively abrogated the suppressive effect of EA at ST36 on the endotoxemic rats, suggesting CB2R was involved in the anti-inflammatory effect of EA. EA pretreatment could enhance CB2R expression, inhibit  $\text{Ca}^{2+}$  influx, and inactivate TLR4/NF- $\kappa$ B signaling, which contributes to the alleviation of LPS-induced inflammation in rats.

**KEY WORDS:** electro-acupuncture; lipopolysaccharide; inflammation; calcium; cannabinoid CB2 receptor; TLR4/NF- $\kappa$ B signaling.

## INTRODUCTION

Inflammation is a protective response to local or systemic microbial invasion or injury, and it is also an important component of the innate immune system, which needs to be

fine-tuned and regulated precisely [1]. On the one hand, different types of inflammatory cytokines including tumor necrosis factor-alpha (TNF- $\alpha$ ), interleukin-1 beta (IL-1 $\beta$ ), and interleukin-6 (IL-6) are produced by activated macrophages/monocytes and other immune cells, as the essential mediators involved in local and systemic

Tao Chen and Yong Xiong contributed equally to this work.

<sup>1</sup> Department of Anatomy, School of Basic Medical Sciences, Hubei University of Chinese Medicine, 1 Huangjiahu West Road, Hongshan District, Wuhan, 430065, China

<sup>2</sup> College of Acupuncture and Moxibustion, Hubei University of Chinese Medicine, Wuhan, 430065, China

<sup>3</sup> School of Basic Medical Sciences, Hubei University of Chinese Medicine, Wuhan, 430065, China

<sup>4</sup> Hubei Provincial Collaborative Innovation Center of Preventive Treatment by Acupuncture and Moxibustion, Hubei University of Chinese Medicine, No. 1 Huangjiahu West Road, Hongshan District, Wuhan, 430065, China

<sup>5</sup> To whom correspondence should be addressed to Nina Yin at Department of Anatomy, School of Basic Medical Sciences, Hubei University of Chinese Medicine, 1 Huangjiahu West Road, Hongshan District, Wuhan, 430065, China. E-mail: yinnina-hbctcm@hotmail.com; and Zebin Chen at Hubei Provincial Collaborative Innovation Center of Preventive Treatment by Acupuncture and Moxibustion, Hubei University of Chinese Medicine, No. 1 Huangjiahu West Road, Hongshan District, Wuhan, 430065, China. E-mail: chenzebin-hbctcm@outlook.com

inflammation [2]. On the other hand, overproduction of inflammatory cytokines leads to excessive cell damage and tissue injury. Once they spread into the bloodstream, dangerous inflammatory responses will be induced and triggered, such as severe, multiorgan failure and even death [3].

Lipopolysaccharide (LPS) is a major component of the cell wall of Gram-negative bacteria and is released once bacterial cell division or death [4]. LPS plays an important role as a prototype microbe-derived activator *via* toll like receptor 4 (TLR4)-dependent signaling, leading to subsequent cascade generation of multiple pro- and anti-inflammatory mediators [5]. The pro-inflammatory action of LPS is crucial for curbing pathogenic microbial infections, but uncontrolled host responses to LPS can incur systemic inflammatory events—endotoxemia, sepsis, and fatal septic shock [6]. The strategy of diminishing inflammation in infectious diseases has attracted increasing attention in recent years. Owing to the advantageous characteristics, including economy, convenience, and few side effects, electro-acupuncture (EA) has been widely applied in animal stroke models and stroke patients [7–9].

EA is derived from traditional Chinese medicine. As a novel therapy based on traditional acupuncture in combination with modern electrotherapy, EA possesses many beneficial properties, such as neuroprotective, anti-diabetic, anti-oxidative, anti-inflammatory, anti-allergic, and anti-apoptotic effects [10]. Our previous study showed that EA at zusanli (ST36) acupoint attenuated allergic skin inflammation in mice, which was associated with the reduction of inflammatory cell infiltration and pro-inflammatory cytokine production, such as interferon-gamma (IFN- $\gamma$ ) and TNF- $\alpha$  [11]. Additionally, EA at ST36 ameliorated allergic contact dermatitis in rats, accompanying the downregulation of inflammatory cytokines including TNF- $\alpha$  and IL-1 $\beta$  [12]. Other studies also indicated that EA pretreatment suppressed LPS-induced endotoxemia and endotoxic shock in rats and rabbits, respectively [13, 14]. However, the underlying mechanisms involved in the anti-inflammatory effect of EA in endotoxemic rats are not yet well defined.

In the present study, we reasoned that EA pretreatment at ST36 played a protective role using a rat model of LPS-induced endotoxemia. Here, the anti-inflammatory effect of EA was associated with enhancement of CB2R expression and inhibition of Ca<sup>2+</sup> influx, contributing to inactivation of TLR4/NF- $\kappa$ B signaling. These findings suggest that EA pretreatment at ST36 might potentially be used as an alternative therapy method to prevent/treat diseases based on inflammation.

## MATERIALS AND METHODS

### Animals

Male 7-week-old Sprague-Dawley rats (200–220 g) were purchased from Hubei Research Center of Laboratory Animals (Wuhan, China) and housed in an air-conditioned room (23  $\pm$  0.5 °C, 12 h light/dark cycle) with free access to food and water. Animal care and use were in accordance with guidelines approved by the Institutional Animal Care and Use Committee of Hubei University of Chinese Medicine (No.: SYXK2012-0067).

### Groups and Experimental Protocols

Rats were randomly divided into five groups ( $n = 5$  per group): Group I (Control), not treated; Group II (EA), electro-acupuncture pretreatment at bilateral zusanli acupoints (ST36) for a week; Group III (LPS), intraperitoneal injection of LPS to induce endotoxemia; Group IV (EA + LPS), EA pretreatment at ST36 for a week, then intraperitoneal injection of LPS after 2 h following the last EA stimulation on day 7. After an additional 2 h, rats were sacrificed and the samples were collected; Group V (AM630 + EA + LPS).

AM630 (specific CB2R antagonist; Sigma-Aldrich, St. Louis, MO, USA) were dissolved in 5% dimethyl sulfoxide before use. Based on previous report [15], the dose for AM630 (1 mg/kg) was chosen in this study and administered intraperitoneally 1 h before EA pretreatment for continuous 7 days.

### EA Pretreatment at Zusanli (ST36) Acupoint

Zusanli (ST36) acupoint is located approximately 5 mm below the fibular head and lateral to the anterior tubercle of the tibia. Electrical stimulation was applied to bilateral ST36 *via* two needles with a Hans Acupoint Nerve Stimulator (HANS, Beijing, China). The needles (length 3.0 cm, diameter 0.20 mm) (Suzhou Medical Appliance Factory, Suzhou, China) were inserted perpendicular to the skin. The following parameters were used: a continuous wave at 2 Hz and 1 mA for 5 min, 2 Hz and 1.5 mA for 5 min, and 2 Hz and 2 mA for 20 min.

### Endotoxemia Model

Rats were injected intraperitoneally with LPS (*Escherichia coli* 0111: B4; 5 mg/kg) (Sigma-Aldrich), dissolved in sterile, pyrogen-free saline that was sonicated for 30 min immediately before use.

### Cytokine Assay by Enzyme-Linked Immunosorbent Assay

Blood samples were collected for cytokine assay with enzyme-linked immunosorbent assay (ELISA) kits (R&D systems, Minneapolis, MN, USA), including TNF- $\alpha$ , IL-1 $\beta$ , and IL-6, according to the manufacturer's instruction. All experiments were done in triplicate.

### Histological Examination of Zusanli Acupoint

The skin tissues of local zusanli acupoint (about 1 cm  $\times$  1 cm  $\times$  1 cm) were obtained and fixed with 4% paraformaldehyde (Sigma-Aldrich). The tissue specimens were embedded in paraffin, cut into 5  $\mu$ m section, and stained with hematoxylin and eosin (H&E) for histological analysis. Pictures were observed and captured using a Nikon Eclipse Ti-S microscope (Nikon, Tokyo, Japan). All sections were randomized and evaluated by two trained observers who were blinded to the groups.

### Detection of Ca<sup>2+</sup> Concentration

To detect Ca<sup>2+</sup> concentration in the local zusanli acupoint, the tissue samples were collected, weighed (80 mg), and homogenized in 1 ml of tissue protein extraction reagent containing a protease inhibitor cocktail (Pierce, Rockford, IL, USA). Homogenates were centrifuged at 12,000 $\times$ g for 15 min at 4 °C to obtain the supernatant. Ca<sup>2+</sup> concentration in ST36 and serum were determined with the BioVision kit (BioVision Inc., Mountain View, CA, USA) using a micro-plate reader (Thermo Scientific, Waltham, MA, USA), respectively. All experiments were done in triplicate.

### Preparation of Spleen Mononuclear Cells

Spleen mononuclear cells were isolated by density gradient centrifugation (2000 rpm/min for 30 min) (Ficoll-Hypaque, density 1.077 g/ml) (Sigma-Aldrich) and incubated overnight at 37 °C in complete RPMI-1640 medium containing 10% fetal bovine serum and antibiotics (100 units/ml streptomycin and penicillin) (Gibco, Grand Island, NY, USA). Next day, non-adherent cells were harvested as spleen mononuclear cells.

### Real-Time RT-PCR

Total RNA of spleen mononuclear cells was extracted using the Trizol reagent (Invitrogen, Carlsbad, CA, USA). Quantitative PCR was performed using the SYBR-Green Master PCR Mix (Applied Biosystems, Foster City, CA,

USA) on the TP800 qPCR System (Takara, Japan). Following the forward (F) and reverse (R) primer sequences were used: CB1R: F, 5'-CTACGTGGGCTCGAATGACA-3'; R, 5'-GACCAACGGGGAGTTGTCTC-3'; CB2R: F, 5'-GCCTGGTCATGGCTGTTCTG-3'; R, 5'-CAGCAGAGCGGATCTCTCCA-3'; GAPDH: F, 5'-CCCCCAATGTATCCGTTGTG-3'; R, 5'-TAGCCCAGGATGCCCTTTAGT-3'. Amplification was performed under the following conditions: 10 min at 95 °C, then 40 cycles of 15 s at 95 °C and 1 min at 60 °C. The relative CB1R/CB2R mRNA levels were normalized to those of GAPDH. Data were analyzed by the 2<sup>- $\Delta\Delta$ Ct</sup> method [16].

### Immunohistochemical Analysis

Briefly, tissue sections of spleen were deparaffinized with xylene and rehydrated through graded series of alcohols. Tissue sections were rinsed in PBS, pretreated with citrate buffer at 93 °C, blocked with 5% normal blocking serum for 1 h, and then incubated with a primary antibody reactive against TLR4 (sc-293072, Santa Cruz Biotechnology Inc., Santa Cruz, CA, USA) for 2 h at room temperature. Washed sections were incubated with secondary rabbit anti-mouse IgG biotin for 30 min. The reaction product was visualized with DAB chromogenic agent. The sections were counterstained with hematoxylin stain. Slides were analyzed using an Olympus BX60 (Olympus Optical Co Ltd., Tokyo, Japan).

### Western Blot

Spleen mononuclear cells were lysed with RIPA Lysis Buffer (Cell Signaling Technology Inc., Beverly, MA, USA). The supernatants were analyzed for protein concentration using a BCA Protein Assay kit (Pierce, Rockford, IL, USA). A total of 20  $\mu$ g protein per lane was separated by 10% SDS-PAGE. Subsequently, blots were transferred onto polyvinylidene difluoride membranes and were blocked for 2 h with 5% non-fat dry milk at room temperature. Membranes were incubated with primary rabbit anti-rat antibodies against CB2R (sc-25494), TLR4 (sc-293072) (Santa Cruz), GAPDH (#5174), NF- $\kappa$ B p65 (#3034), Lamin B1(#13435) (Cell Signaling Technology Inc., Beverly, MA, USA), overnight at 4 °C, followed by incubation with the appropriate HRP-conjugated secondary antibody (Santa Cruz). The bands were visualized by enhanced chemiluminescence detection (HP Scanjet 7400C) (Hewlett-Packard Co., Palo Alto, CA, USA). Optical density for each band was assessed using ImageJ analysis software (National Institutes of Health, Bethesda,

MD, USA). Sample loading was normalized by quantities of GAPDH or Lamin B1 detected parallel.

### Measurement of $\text{Ca}^{2+}$ Influx

Ratiometric imaging of intracellular  $\text{Ca}^{2+}$  using cells loaded with fura-2/AM was measured as previously described [17]. Briefly, spleen mononuclear cells were isolated and washed three times with Tyrode's buffer. Then, the cells were co-incubated with fura-2/AM (2  $\mu\text{M}$  final concentration) (Invitrogen) at 37 °C for 30 min. After discarding fura-2/AM, the cells were resuspended in Tyrode's buffer. Measurement of  $\text{Ca}^{2+}$  influx was made using a Leica DMI 6000B fluorescence microscope controlled by the SlideBook software (Intelligent Imaging Innovations; Denver, CO, USA). Fluorescence emission at 505 nm was monitored while alternating excitation wavelengths between 340 and 380 nm at a frequency of 0.5 Hz.  $\text{Ca}^{2+}$  influx was shown as 340/380 nm ratio.

### Statistical Analysis

Data were presented as the mean  $\pm$  standard deviation (SD). Results were analyzed with SPSS 19.0 software (SPSS Inc., Chicago, IL, USA). For comparisons of multiple samples, one-way analysis of variance (ANOVA) was

used. For comparisons between two groups, a Student's *t* test was used. Curve estimation and linear regression analyses were performed for correlation analysis.  $P < 0.05$  indicated statistical significance.

## RESULTS

### EA Pretreatment at ST36 Attenuates LPS-Induced Inflammation in Rats

Firstly, we observed the effect of EA pretreatment at ST36 on LPS-induced inflammation using a rat model of endotoxemia (Fig. 1a). LPS injection (5 mg/kg, i.p.) evoked apparently an inflammatory response characterized by the increased production of inflammatory cytokines, such as TNF- $\alpha$ , IL-1 $\beta$ , and IL-6. However, EA pretreatment at ST36 strongly inhibited the levels of pro-inflammatory cytokines in serum (Fig. 1b-d).

### EA Pretreatment Lowers $\text{Ca}^{2+}$ Concentration in Endotoxemic Rats

Next, we investigated histological changes of the local zusanli acupoint. As shown in Fig. 2a, there was no obvious difference in dermis thickness, inflammatory cell

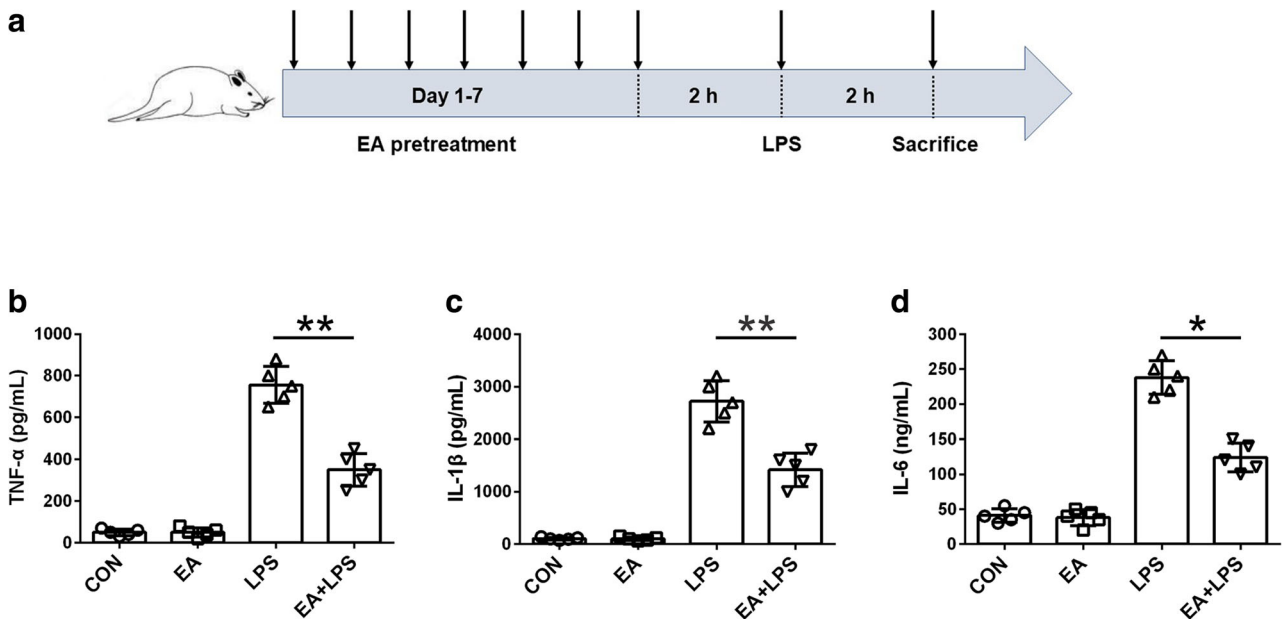


**Fig. 1.** EA pretreatment at ST36 attenuates LPS-induced inflammation in rats. **a** Schematic diagram of the experimental procedure. Rats were treated with a 7-day continuous EA stimulation at the bilateral ST36 acupoints. Then, intraperitoneal injection of LPS was performed after 2 h following the last EA treatment on day 7. After an additional 2 h, rats were sacrificed and the samples were collected. **b–d** Cytokine production in serum was measured by ELISA, including TNF- $\alpha$ , IL-1 $\beta$ , and IL-6. Data are presented as mean  $\pm$  SD ( $n = 5$ , \* $P < 0.05$  and \*\* $P < 0.01$ ).

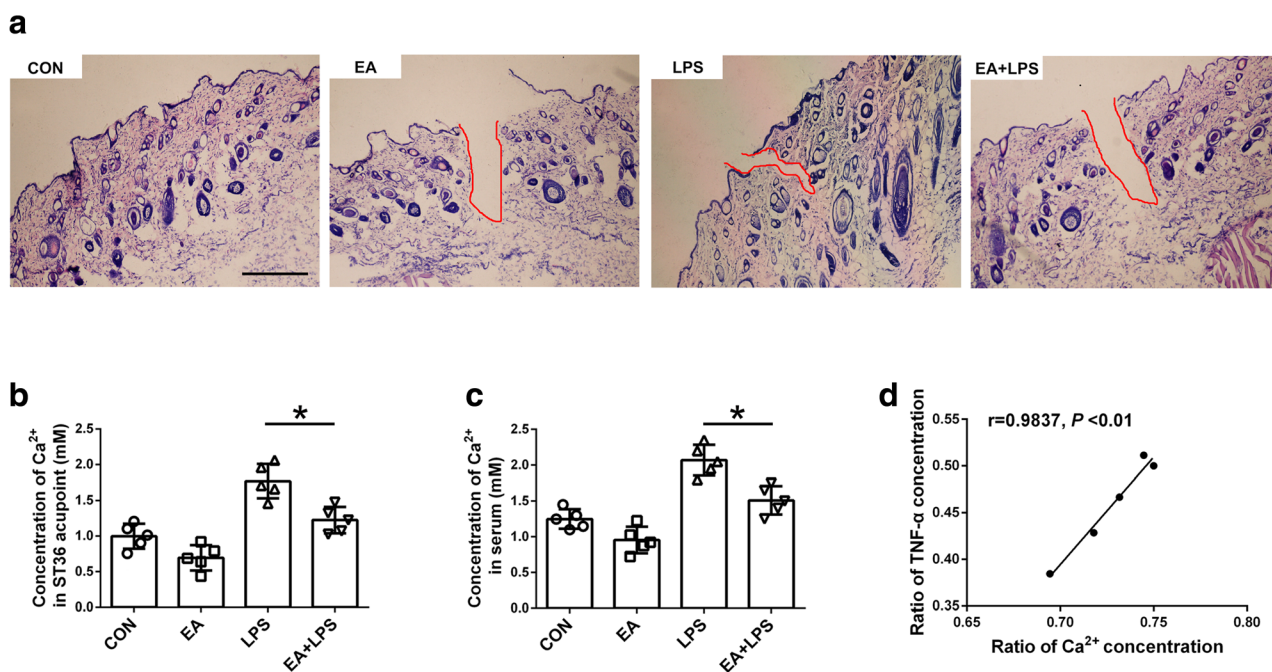


**Fig. 2.** EA pretreatment reduces  $\text{Ca}^{2+}$  concentration in the endotoxemic rats. At the end of the experiment, local zusanli acupoint tissues and serum of different groups were collect. **a** Histological changes of the local zusanli acupoint were shown using hematoxylin and eosin (H&E) staining. Scale bar = 20  $\mu\text{m}$ . Red curve around area indicated the needle track. **b**  $\text{Ca}^{2+}$  concentration in the local zusanli acupoint and **c** serum of the rats in each group was detected, respectively. **d** Correlation analysis between ratio of  $\text{Ca}^{2+}$  concentration (EA + LPS group / LPS group) and ratio of TNF- $\alpha$  concentration (EA + LPS group / LPS group). Data are presented as mean  $\pm$  SD ( $n=5$ ,  $*P<0.05$ ).

infiltration, and the sebaceous gland hyperplasia. Interestingly,  $\text{Ca}^{2+}$  concentration in the local zusanli acupoint and the serum were decreased in EA + LPS group compared with those in LPS group (Fig. 2b, c). Correlation analysis indicated that the ratio of  $\text{Ca}^{2+}$  concentration (EA + LPS group / LPS group) was positive correlation with the change of TNF- $\alpha$  concentration (EA + LPS group / LPS group) (Fig. 2d), suggesting the downregulation of  $\text{Ca}^{2+}$  levels was associated with the anti-inflammatory effect of EA pretreatment.

#### EA Pretreatment Inhibits $\text{Ca}^{2+}$ Influx and Hampers TLR4/NF- $\kappa\text{B}$ Signaling

Previous studies showed that increased  $\text{Ca}^{2+}$  influx and activated TLR4/NF- $\kappa\text{B}$  signaling participated in LPS-induced inflammation [18, 19]. We speculated that EA pretreatment could hinder  $\text{Ca}^{2+}$  influx and curb TLR4/NF- $\kappa\text{B}$  signaling. Compared to sole LPS administration, EA pretreatment evidently inhibited  $\text{Ca}^{2+}$  influx (Fig. 3a, b), which was consistent with downregulation of extracellular  $\text{Ca}^{2+}$  concentration in the serum. In addition, immunohistochemical analysis exhibited that EA at ST36

suppressed TLR4 expression in the spleen (Fig. 4a). Using the spleen mononuclear cells, western blot showed that EA pretreatment effectively hampered the activation of TLR4/NF- $\kappa\text{B}$  signaling (Fig. 4b–d).

#### EA Pretreatment Enhances CB2R Expression in Endotoxemic Rats

Furthermore, we checked the effect of EA pretreatment on CBR expression, including CB1R and CB2R. LPS application had no obvious effect on CB1R at mRNA and protein levels (data not shown). It was worth noting that EA pretreatment could induce CB2R expression compared with Control group (Fig. 5a–c), which suggested that CB2R might be involved in the anti-inflammatory effect of EA on endotoxemic rats.

#### CB2R Participates in the Anti-inflammatory Activity of EA Pretreatment at ST36 on LPS-Induced Endotoxemia

Lastly, we investigated the anti-inflammatory activity of EA utilizing AM630, a specific CB2R antagonist. As shown in Fig. 6a, AM630 significantly abrogated the

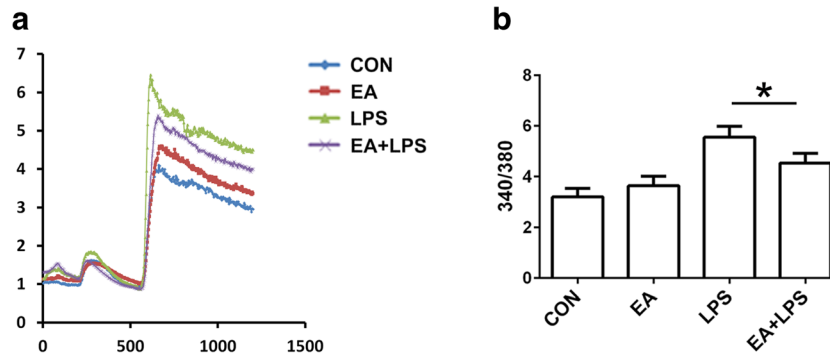


**Fig. 3.** EA pretreatment inhibits  $\text{Ca}^{2+}$  influx. **a** Spleen mononuclear cells were isolated, and  $\text{Ca}^{2+}$  influx was determined and **b** statistically analyzed. Representative traces of intracellular  $\text{Ca}^{2+}$  changes were observed. Data are presented as mean  $\pm$  SD ( $n = 5$ ,  $*P < 0.05$ ).

suppressive effect of EA pretreatment on  $\text{TNF-}\alpha$  production and  $\text{Ca}^{2+}$  concentration in the serum (Fig. 6a, b). Additionally, AM630 distinctly dampened the inhibitive effect of EA on TLR4/NF- $\kappa$ B signaling (Fig. 6c–e). Simultaneously, the inhibition of  $\text{Ca}^{2+}$  influx accompanying EA

pretreatment was also reversed in response to AM630 (Fig. 6f, g). These findings suggested that CB2R participated in inhibiting  $\text{Ca}^{2+}$  influx and inactivating TLR4/NF- $\kappa$ B signaling associated with the anti-inflammatory effect of EA pretreatment at ST36 on LPS-induced endotoxemia.

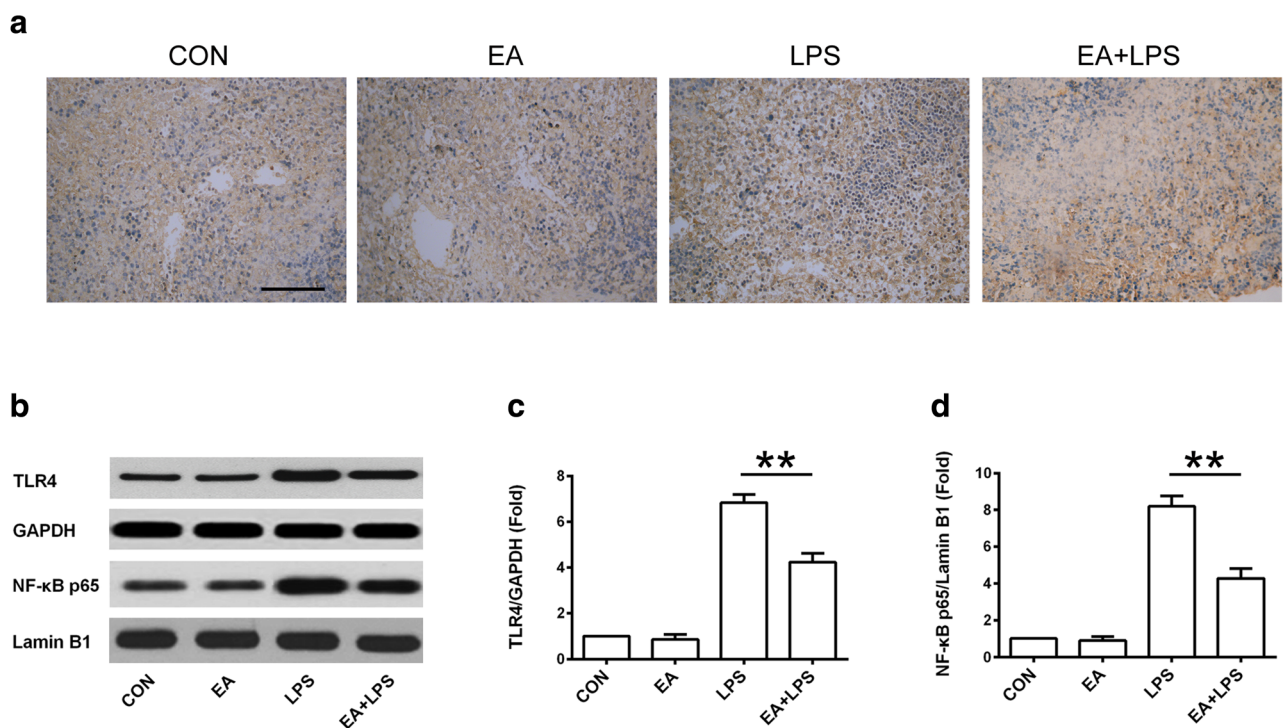


**Fig. 4.** EA pretreatment suppresses TLR4/NF- $\kappa$ B signaling. **a** TLR4 expression in the spleen was assayed by immunohistochemical analysis. The positive signal is brown or dark brown. Scale bar = 20  $\mu$ m. **b** TLR4 and NF- $\kappa$ B (p65) expression at protein level were detected *via* western blot, and the representative results were shown. **c** Statistical analysis of the relative expression of TLR4 and **d** NF- $\kappa$ B (p65) was shown, respectively. Data are presented as mean  $\pm$  SD ( $n = 5$ ,  $**P < 0.01$ ).

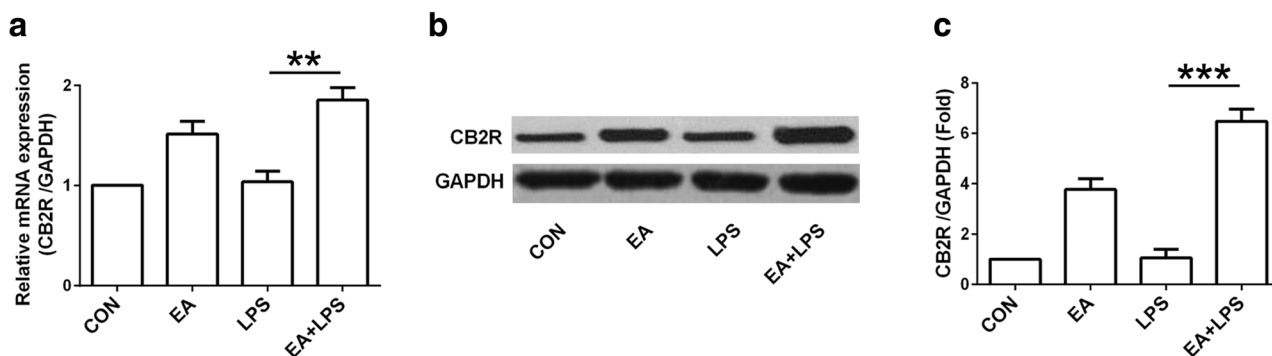


**Fig. 5.** EA pretreatment enhances CB2R expression in the endotoxemic rats. **a** Spleen mononuclear cells were isolated, CB2R expression at mRNA level was measured by real-time PCR and statistically analyzed. **b** CB2R expression at protein level was detected *via* western blot, and a representative result was shown. **c** Statistical analysis of the relative expression of CB2R in the different group was shown. Data are presented as mean  $\pm$  SD ( $n = 5$ ,  $**P < 0.01$  and  $***P < 0.001$ ).

## DISCUSSION

This study was conducted to investigate the effect of EA pretreatment at ST36 in LPS-induced inflammation using the endotoxemic rat model and to explore the potential mechanisms. Our results demonstrated that the inhibition of  $Ca^{2+}$  influx accompanying enhancement of CB2R expression participated in the anti-inflammatory effect of EA pretreatment, which contributed to the involvement of inactivating TLR4/NF- $\kappa$ B signaling in the molecular mechanisms.

As an important actor in inflammation, TNF- $\alpha$  can initiate other pro-inflammatory cytokines, such as IL-1 $\beta$  and IL-6, and amplify other inflammatory mediators [20]. Increasing evidence indicates the anti-endotoxemic effect of EA pretreatment following LPS application in experimental animals, in which the reduction of inflammatory cytokine production was presented [21–23]. Similar with these reporters, EA pretreatment at ST36 in this study also showed the ability to curb the synthesis and release of TNF- $\alpha$ , IL-1 $\beta$ , and IL-6 (Fig. 1b–d). However, there were no significant difference in histological changes of local ST36 acupoint, such as skin swelling, inflammatory cell infiltration, and angiogenesis (Fig. 2a). Then, a central question rising was that how EA stimulation at ST36 affect the systemic inflammation induced by LPS administration.

A previous study showed that intracellular  $Ca^{2+}$  might play an important role in low-frequency EA analgesia by modulating the phosphorylation state of the spinal N-methyl-d-aspartate receptor (NMDAR) subunits [24]. EA pretreatment could produce anti-arrhythmic effect in the rats subjected to simulative global ischemia and reperfusion (SGIR), which was due at least partially to the inhibition of SGIR-induced  $Ca^{2+}$  overload and intracellular  $Ca^{2+}$

oscillations [25]. Our recent publication revealed that EA treatment could reduce  $Ca^{2+}$  concentration in serum of normal rats [26]. Consistent with the decrement of  $Ca^{2+}$  concentration in the serum, EA pretreatment also lowered the levels of  $Ca^{2+}$  in local acupoint (Fig. 2b, c). The ration of  $Ca^{2+}$  concentration was positive correlation with the change of TNF- $\alpha$  production (Fig. 2d), suggesting its possible role of  $Ca^{2+}$  as a mediator in the severity of inflammation. These findings suggest that the change of  $Ca^{2+}$  influx maybe play a connective role as a bridge of communication between local EA stimulation and systemic effect in the endotoxemic rats.

Since the identification of TLR4 as the LPS receptor, it has long been assumed to trigger intracellular signal responses following cascade of events starting from an interaction, which activates p65 nuclear factor of kappa light chain enhancer in B cells (NF- $\kappa$ B) through different pathway, resulting in the expression of genes related to inflammation [27]. A recent study showed that  $Ca^{2+}$ /calmodulin-dependent Akt activation played an important role in LPS-induced NF- $\kappa$ B activation, suggesting the relationship between the change of  $Ca^{2+}$  and NF- $\kappa$ B activation [28]. Following the reduction of  $Ca^{2+}$  concentration in the overall level after EA pretreatment (Fig. 3a, b), the expression of TLR4 and NF- $\kappa$ B p65 proteins was also downregulated (Fig. 4a–d). These results further emphasized the central role of  $Ca^{2+}$  in the biological effect of EA stimulation. If the change of  $Ca^{2+}$  concentration in local acupoint elicits the nerve impulse conduction, or  $Ca^{2+}$  flow as transmitter affects the activation of neuro-endocrine-immune system, or  $Ca^{2+}$  initiates other suppressive mechanism such as vagal- and  $\alpha 7nAChR$ -dependent cholinergic anti-inflammatory pathways, further studies are needed to clarify the facts.

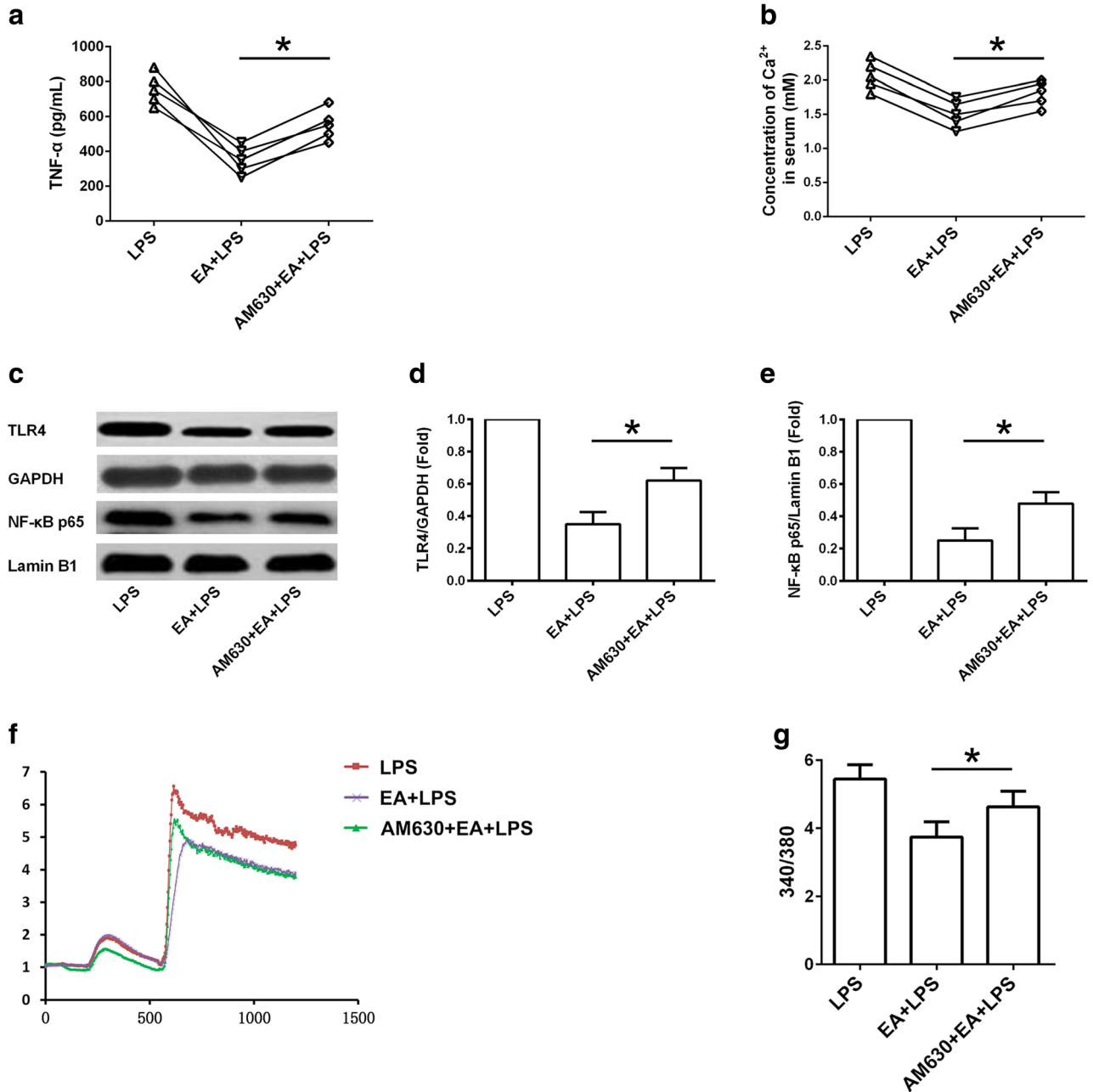


**Fig. 6.** CB2R is involved in the anti-inflammatory effect EA pretreatment in the endotoxemic rats. **a** Following AM630 administration, TNF- $\alpha$  production in the serum was measured by ELISA. **b** The concentrations of Ca<sup>2+</sup> in the serum from different groups were detected. **c** The expression of TLR4 and NF- $\kappa$ B (p65) proteins were detected by western blot, and the representative results were shown. **d** Statistical analysis of the relative expression of TLR4 and **e** NF- $\kappa$ B (p65) was shown, respectively. **f** Spleen mononuclear cells were isolated, and Ca<sup>2+</sup> influx was determined and **g** statistically analyzed. Representative traces of intracellular Ca<sup>2+</sup> changes were observed. Data are presented as mean  $\pm$  SD ( $n = 5$ ,  $*P < 0.05$ ).

Different with CB1R named as the “central” cannabinoid receptor, CB2R is referred to as the “peripheral” cannabinoid receptor because they are

mostly found on the immune cells [29]. Previous studies showed that EA treatment stimulated and increased CB2R expression in inflamed tissues [30, 31]. A latest

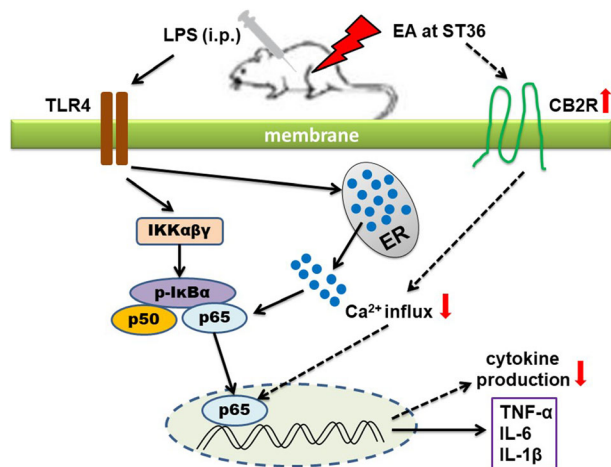


**Fig. 7.** Proposed mechanism for the anti-inflammatory activity of EA pretreatment at ST36 on LPS-induced endotoxemia. EA pretreatment at ST36 prompts CB2R expression and inhibits Ca<sup>2+</sup> influx, resulting in subsequent inactivation of TLR4/NF-κB signaling, which contributes to the anti-inflammatory effect of EA pretreatment at ST36 on LPS-induced endotoxemia.

study reported that CB2 receptors were involved in the analgesic effect of EA on inflammatory pain. Stimulation of CB2 receptors inhibited inflammasome activation in inflamed skin tissues [32]. In addition, EA at Huantiao (GB30) and Yanglingquan (GB34) acupoints reduced inflammatory pain through CB2R activation, which was significantly attenuated with the application of CB2R antagonist AM630. Conversely, CB2R agonist AM1242 produced analgesia similar with EA treatment, and the effect was also blocked by AM630 [33]. Our results showed EA pretreatment enhanced CB2R expression at mRNA and protein levels (Fig. 5a–c). Importantly, CB2R antagonist AM630 reversed the anti-endotoxemic effect of EA (Fig. 6), which strongly suggested that CB2R activation was beneficial to EA pretreatment in the endotoxemic rats.

Based on previous studies and our present results, we speculate that EA pretreatment at ST36 can reduce Ca<sup>2+</sup> influx through activating CB2R in local acupoint, and hamper subsequently the activation of TLR4/NF-κB signaling, resulting in the inhibition of LPS-induced inflammation in rats (Fig. 7). Although further investigations are needed to explain clearly the detailed signal cascades underlying the CB2R-Ca<sup>2+</sup> axis and the downward events, the present study supports EA pretreatment at ST36 as a promising therapeutic strategy for the treatment of several diseases and conditions characterized by inflammation.

## AUTHOR'S CONTRIBUTIONS

Tao Chen, Yong Xiong, Nina Yin, and Zebin Chen designed the study; Tao Chen and Yong Xiong performed the experiments and wrote the manuscript; Man Long and Dan Zheng contributed to the rat model and EA pretreatment; Hui Ke helped analyze the data; and Jun Xie and Zebin Chen revised the manuscript.

## FUNDING

This study was supported by the grants from the Health and Family Planning Commission of Hubei Province (No. 2013Z-Z01) and the Natural Science Foundation of Hubei Province of China (No. 2015CFA096).

## COMPLIANCE WITH ETHICAL STANDARDS

**Conflicts of Interest.** The authors declare that they have no conflicts of interest.

## REFERENCES

- Tracey, K.J. 2002. The inflammatory reflex. *Nature* 420: 853–859.
- Schett, G., D. Elewaut, I.B. McInnes, J.M. Dayer, and M.F. Neurath. 2013. How cytokine networks fuel inflammation: toward a cytokine-based disease taxonomy. *Nature Medicine* 19: 822–824.
- Headland, S.E., and L.V. Norling. 2015. The resolution of inflammation: principles and challenges. *Seminars in Immunology* 27: 149–160.
- Raetz, C.R., and C. Whitfield. 2002. Lipopolysaccharide endotoxins. *Annual Review of Biochemistry* 71: 635–700.
- Plóciennikowska, A., A. Hromada-Judycka, K. Borzęcka, and K. Kwiatkowska. 2015. Co-operation of TLR4 and raft proteins in LPS-induced pro-inflammatory signaling. *Cellular and Molecular Life Sciences* 72: 557–581.
- Opal, S.M. 2010. Endotoxins and other sepsis triggers. *Contributions to Nephrology* 167: 14–24.
- Xue, X., Y. You, J. Tao, X. Ye, J. Huang, S. Yang, Z. Lin, Z. Hong, J. Peng, and L. Chen. 2014. Electro-acupuncture at points of zusanli and quchi exerts anti-apoptotic effect through the modulation of PI3K/Akt signaling pathway. *Neuroscience Letters* 558: 14–19.
- Lu, Y., H. Zhao, Y. Wang, B. Han, T. Wang, H. Zhao, K. Cui, and S. Wang. 2015. Electro-acupuncture up-regulates astrocytic MCT1 expression to improve neurological deficit in middle cerebral artery occlusion rats. *Life Sciences* 134: 68–72.
- Youn, J.I., K.K. Sung, B.K. Song, M. Kim, and S. Lee. 2013. Effects of electro-acupuncture therapy on post-stroke depression in patients with different degrees of motor function impairments: a pilot study. *Journal of Physical Therapy Science* 25: 725–728.
- Fukazawa, Y., T. Maeda, and S. Kishioka. 2009. The pharmacological mechanisms of electroacupuncture. *Current Opinion in Investigational Drugs* 10: 62–69.

11. Wang, Z., T. Chen, M. Long, L. Chen, L. Wang, N. Yin, and Z. Chen. 2017. Electro-acupuncture at acupoint ST36 ameliorates inflammation and regulates Th1/Th2 balance in delayed-type hypersensitivity. *Inflammation* 40: 422–434.
12. Wang, Z., T. Yi, M. Long, Y. Gao, C. Cao, C. Huang, Q. Wang, N. Yin, and Z. Chen. 2017. Electro-acupuncture at zusanli acupoint (ST36) suppresses inflammation in allergic contact dermatitis via triggering local IL-10 production and inhibiting p38 MAPK activation. *Inflammation* 40: 1351–1364.
13. Liu, H.W., M.C. Liu, C.M. Tsao, M.H. Liao, and C.C. Wu. 2011. Electro-acupuncture at 'Neiguan' (PC6) attenuates liver injury in endotoxaemic rats. *Acupuncture in Medicine* 29: 284–288.
14. Zhang, Y., J.B. Yu, X.Q. Luo, L.R. Gong, M. Wang, X.S. Cao, S.A. Dong, Y.M. Yan, Y. Kwon, and J. He. 2014. Effect of ERK1/2 signaling pathway in electro-acupuncture mediated up-regulation of heme oxygenase-1 in lungs of rabbits with endotoxin shock. *Medical Science Monitor* 20: 1452–1460.
15. Liu, Z., X. Chen, Y. Gao, S. Sun, L. Yang, Q. Yang, F. Bai, L. Xiong, and Q. Wang. 2015. Involvement of GluR2 up-regulation in neuro-protection by electroacupuncture pretreatment via cannabinoid CB1 receptor in mice. *Scientific Reports* 5: 9490.
16. Schmittgen, T.D., and K.J. Livak. 2008. Analyzing real-time PCR data by the comparative C(T) method. *Nature Protocols* 3: 1101–1108.
17. Yin, N., X. Hong, Y. Han, Y. Duan, Y. Zhang, and Z. Chen. 2015. Cortex Mori Radicis extract induces neurite outgrowth in PC12 cells activating ERK signaling pathway via inhibiting Ca<sup>2+</sup> influx. *International Journal of Clinical and Experimental Medicine* 8: 5022–5032.
18. Schappe, M.S., K. Sztayn, M.E. Stremaska, S.K. Mendu, T.K. Downs, P.V. Seegren, M.A. Mahoney, S. Dixit, J.K. Krupa, E.J. Stipes, J.S. Rogers, S.E. Adamson, N. Leitinger, and B.N. Desai. 2018. Chanzyme TRPM7 mediates the Ca<sup>2+</sup> influx essential for lipopolysaccharide-induced Toll-like receptor 4 endocytosis and macrophage activation. *Immunity* 48: 59–74.e5.
19. Zhang, Y., Y. Lu, L. Ma, X. Cao, J. Xiao, J. Chen, S. Jiao, Y. Gao, C. Liu, Z. Duan, D. Li, Y. He, B. Wei, and H. Wang. 2014. Activation of vascular endothelial growth factor receptor-3 in macrophages restrains TLR4-NF- $\kappa$ B signaling and protects against endotoxin shock. *Immunity* 40: 501–514.
20. Olmos, G., and J. Lladó. 2014. Tumor necrosis factor alpha: a link between neuroinflammation and excitotoxicity. *Mediators of Inflammation* 2014: 861231.
21. Song, Q., S. Hu, H. Wang, Y. Lv, X. Shi, Z. Sheng, and W. Sheng. 2014. Electroacupuncture at zusanli point (ST36) attenuates pro-inflammatory cytokine release and organ dysfunction by activating cholinergic anti-inflammatory pathway in rat with endotoxin challenge. *African Journal of Traditional, Complementary, and Alternative Medicines* 11: 469–474.
22. Yu, J.B., S.A. Dong, X.Q. Luo, L.R. Gong, Y. Zhang, M. Wang, X.S. Cao, and D.Q. Liu. 2013. Role of HO-1 in protective effect of electro-acupuncture against endotoxin shock-induced acute lung injury in rabbits. *Experimental Biology and Medicine (Maywood, N.J.)* 238: 705–712.
23. Park, J.Y., and U. Namgung. 2018. Electroacupuncture therapy in inflammation regulation: current perspectives. *Journal of Inflammation Research* 11: 227–237.
24. Jung, T.G., J.H. Lee, I.S. Lee, and B.T. Choi. 2010. Involvement of intracellular calcium on the phosphorylation of spinal N-methyl-D-aspartate receptor following electroacupuncture stimulation in rats. *Acta Histochemica* 112: 127–132.
25. Gao, J., Y. Zhao, Y. Wang, J. Xin, J. Cui, S. Ma, F. Lu, L. Qin, and X. Yu. 2015. Anti-arrhythmic effect of acupuncture pretreatment in the rats subjected to simulative global ischemia and reperfusion—involve-ment of intracellular Ca<sup>2+</sup> and connexin 43. *BMC Complementary and Alternative Medicine* 15: 5.
26. Chen, L., A. Xu, N. Yin, M. Zhao, Z. Wang, T. Chen, Y. Gao, and Z. Chen. 2017. Enhancement of immune cytokines and splenic CD4<sup>+</sup> T cells by electroacupuncture at ST36 acupoint of SD rats. *PLoS One* 12: e0175568.
27. Mittal, M., C. Tiruppathi, S. Nepal, Y.Y. Zhao, D. Grzych, D. Soni, D.J. Prockop, and A.B. Malik. 2016. TNF $\alpha$ -stimulated gene-6 (TSG6) activates macrophage phenotype transition to prevent inflammatory lung injury. *Proceedings of the National Academy of Sciences of the United States of America* 113: E8151–E8158.
28. Zhou, X., W. Yang, and J. Li. 2006. Ca<sup>2+</sup>- and protein kinase C-dependent signaling pathway for nuclear factor-kappaB activation, inducible nitric-oxide synthase expression, and tumor necrosis factor-alpha production in lipopolysaccharide-stimulated rat peritoneal macrophages. *The Journal of Biological Chemistry* 281: 31337–31347.
29. Toczek, M., and B. Malinowska. 2018. Enhanced endocannabinoid tone as a potential target of pharmacotherapy. *Life Sciences* 204: 20–45.
30. Chen, L., J. Zhang, F. Li, Y. Qiu, L. Wang, Y.H. Li, J. Shi, H.L. Pan, and M. Li. 2009. Endogenous anandamide and cannabinoid receptor-2 contribute to electroacupuncture analgesia in rats. *The Journal of Pain* 10: 732–739.
31. Zhang, J., L. Chen, T. Su, F. Cao, X. Meng, L. Pei, J. Shi, H.L. Pan, and M. Li. 2010. Electroacupuncture increases CB2 receptor expression on keratinocytes and infiltrating inflammatory cells in inflamed skin tissues of rats. *The Journal of Pain* 11: 1250–1258.
32. Gao, F., H.C. Xiang, H.P. Li, M. Jia, X.L. Pan, H.L. Pan, and M. Li. 2018. Electroacupuncture inhibits NLRP3 inflammasome activation through CB2 receptors in inflammatory pain. *Brain, Behavior, and Immunity* 67: 91–100.
33. Su, T.F., Y.Q. Zhao, L.H. Zhang, M. Peng, C.H. Wu, L. Pei, B. Tian, J. Zhang, J. Shi, H.L. Pan, and M. Li. 2012. Electroacupuncture reduces the expression of proinflammatory cytokines in inflamed skin tissues through activation of cannabinoid CB2 receptors. *European Journal of Pain* 16: 624–635.